

Finite-volume methods for non-linear elasticity in heterogeneous media

Randall J. LeVeque*

*Department of Applied Mathematics, University of Washington, Box 352420, Seattle,
WA 98195-2420, U.S.A.*

SUMMARY

An approximate Riemann solver is developed for the equations of non-linear elasticity in a heterogeneous medium, where each grid cell has an associated density and stress–strain relation. The non-linear flux function is spatially varying and a wave decomposition of the flux difference across a cell interface is used to approximate the wave structure of the Riemann solution. This solver is used in conjunction with a high-resolution finite-volume method using the CLAWPACK software. As a test problem, elastic waves in a periodic layered medium are studied. Dispersive effects from the heterogeneity, combined with the non-linearity, lead to solitary wave solutions that are well captured by the numerical method. Copyright © 2002 John Wiley & Sons, Ltd.

1. INTRODUCTION

High-resolution finite-volume methods were originally developed for capturing shock waves in solutions to non-linear systems of conservation laws, such as the Euler equations of gas dynamics. However, they are also well suited to solving both linear and non-linear wave propagation problems in heterogeneous media containing many sharp interfaces where coefficients in the equation have discontinuities. Recently the wave-propagation algorithms described in Reference [1] and implemented in the CLAWPACK software package [2] have been applied to several problems of acoustic or elastic wave propagation in heterogeneous media, e.g. [3, 4].

In this paper these methods are applied to one-dimensional non-linear elastic waves in a heterogeneous medium where each grid cell can have a distinct value of the density ρ_i and its own stress–strain relation $\sigma_i(\varepsilon)$. An approximate Riemann solver for these equations is derived and then applied to a simple but interesting test problem, a periodic medium consisting of alternating thin layers of two different materials. The fine-scale structure gives a dispersive effect that leads to the breakdown of shock waves into oscillations that, in some cases, separate into a train of solitary waves, similar to what is observed for the small-dispersion limit of the

*Correspondence to: R. J. LeVeque, Department of Applied Mathematics, University of Washington, Box 352420, Seattle, WA 98195-2420, U.S.A.

Contract/grant sponsor: DOE; contract/grant number: DE-FG03-96ER 25292
Contract/grant sponsor: NSF; contract/grant number: DMS-9803442

Korteweg–DeVries (KdV) equation. Grid refinement studies show that the method maintains good accuracy on this problem, yielding a useful tool for exploring non-linear phenomena.

The approximate Riemann solver is derived using a technique that is more generally applicable to conservation laws of the form

$$q_t + f(q, x)_x = 0 \quad (1)$$

with a spatially varying flux function $f(q, x)$. The Riemann problem between cells $i - 1$ and i is based on two flux functions $f_{i-1}(q)$ and $f_i(q)$ along with data Q_{i-1} and Q_i . In the case considered here, there are always two propagating wave in the Riemann solution, one wave \mathcal{W}^1 propagating to the left with some speed $s^1 < 0$ and the other wave \mathcal{W}^2 with positive speed s^2 . These are taken to be of the form $\mathcal{W}^1 = \alpha^1 r^1$ and $\mathcal{W}^2 = \alpha^2 r^2$, where the vectors r^1 and r^2 are some presumed ‘wave forms’ and α^1 and α^2 are scalar coefficients. In the linear constant-coefficient case r^1 and r^2 are just the eigenvectors of the coefficient matrix. Approximate Riemann solvers such as Roe’s solver for non-linear problems are based on using eigenvectors of some linearized problem. We take a similar approach here for the spatially varying flux, but with one essential difference. Rather than determining α^1 and α^2 by solving the linear system $Q_i - Q_{i-1} = \alpha^1 r^1 + \alpha^2 r^2$, we instead solve the system $f_i(Q_i) - f_{i-1}(Q_{i-1}) = \beta^1 r^1 + \beta^2 r^2$ and then define $\alpha^p = \beta^p / s^p$ for $p = 1, 2$. This is natural because the flux must be continuous at the interface, whereas q will typically have a jump there, corresponding to stationary waves that are not included in the wave decomposition.

This same approach has proved useful for other problems with spatially-varying fluxes, and is discussed in more detail in Reference [5]. In particular, it has been used to deal with spatial variation that arises when a conservation-law is solved on a general manifold [6], such as those arising in general relativity [7]. This approach can also be related to the relaxation scheme of Jin and Xin [11] and this connection is explored in Reference [8].

2. ELASTICITY EQUATIONS

We consider the one-dimensional elastic wave equation for compressional waves, which have the form

$$\begin{aligned} \varepsilon_t(x, t) - u_x(x, t) &= 0 \\ (\rho(x)u(x, t))_t - \sigma(\varepsilon(x, t), x)_x &= 0 \end{aligned} \quad (2)$$

where $\varepsilon(x, t)$ is the strain, $u(x, t)$ the velocity, $\rho(x)$ the density and $\sigma(\varepsilon, x)$ the stress. We also use $m = \rho u$ to denote the momentum. We allow the stress–strain relationship (along with ρ) to vary in a specified manner with x to represent a heterogeneous medium. This is a non-linear conservation law of form (1) where

$$q(x, t) = \begin{bmatrix} \varepsilon \\ \rho u \end{bmatrix} = \begin{bmatrix} \varepsilon \\ m \end{bmatrix}, \quad f(q, x) = \begin{bmatrix} -m/\rho(x) \\ -\sigma(\varepsilon, x) \end{bmatrix} \quad (3)$$

For sufficiently small deformations we can assume a linear stress–strain relation of the form

$$\sigma(\varepsilon, x) = K(x)\varepsilon$$

where $K(x)$ is the bulk modulus of compressibility. In this case the linear hyperbolic system has the coefficient matrix

$$A = \begin{bmatrix} 0 & -1/\rho \\ -K & 0 \end{bmatrix} \quad (4)$$

with eigenvalues $\lambda^1 = -c$ and $\lambda^2 = c$, where $c = \sqrt{K/\rho}$ is the sound speed. The corresponding eigenvectors are

$$r^1 = \begin{bmatrix} 1 \\ Z \end{bmatrix}, \quad r^2 = \begin{bmatrix} 1 \\ -Z \end{bmatrix} \quad (5)$$

where $Z = \rho c$ is the impedance. In the linear case it is also possible to rewrite the equations by eliminating ε and using $p = -\sigma$ to obtain

$$\begin{aligned} p_t + K(x)u_x &= 0 \\ \rho(x)u_t + p_x &= 0 \end{aligned} \quad (6)$$

These are the equations of one-dimensional linear acoustics in a heterogeneous medium, as used in References [1, 4] for example. For non-linear problems it is better to use the conservative form (2).

Our goal is to apply the high-resolution wave-propagation algorithms described in Reference [1] to this system, and more specifically the `CLAWPACK` software package [2]. To do so we need to only provide a Riemann solver for the system (2). We assume each finite-volume grid cell has associated with it a density ρ_i and a stress-strain relation $\sigma_i(\varepsilon)$. The Riemann problem at $x_{i-1/2}$ between cells $i-1$ and i then consists of Equations (2) with

$$\rho(x) = \begin{cases} \rho_{i-1} & \text{if } x < x_{i-1/2} \\ \rho_i & \text{if } x > x_{i-1/2} \end{cases}, \quad \sigma(\varepsilon, x) = \begin{cases} \sigma_{i-1}(\varepsilon) & \text{if } x < x_{i-1/2} \\ \sigma_i(\varepsilon) & \text{if } x > x_{i-1/2} \end{cases} \quad (7)$$

and arbitrary data Q_{i-1} and Q_i . The solution to this Riemann problem consists in general of two waves (shock or rarefaction waves if the $\sigma(\varepsilon)$ are non-linear functions), one moving to the left into cell $i-1$ and one moving to the right into cell i . Each wave is confined entirely to one material and hence is a standard shock or rarefaction wave relative to that material. This follows from the fact that these equations are expressed in a Lagrangian frame (the spatial variable x represents location relative to a fixed reference configuration) and so the characteristic speeds never cross zero. In particular, there can be no transonic rarefaction waves for these equations. This is convenient since one can then develop an approximate Riemann solver based entirely on shock waves (or approximations to these shocks) and rely on numerical viscosity to give the correct entropy-satisfying solution, without the need for an ‘entropy fix’.

Figure 1 indicates the structure of the all-shock Riemann solution for this problem. The left-going shock, indicated by \mathcal{W}^1 , propagates at a speed s^1 and connects Q_{i-1} to a state Q_{i-1}^* . The jumps across the wave must satisfy the Rankine–Hugoniot conditions

$$\begin{aligned} s^1(\varepsilon_{i-1}^* - \varepsilon_{i-1}) &= -(u_{i-1}^* - u_{i-1}) \\ s^1(\rho_{i-1}u_{i-1}^* - \rho_{i-1}u_{i-1}) &= -(\sigma_{i-1}(\varepsilon_{i-1}^*) - \sigma_{i-1}(\varepsilon_{i-1})) \end{aligned} \quad (8)$$

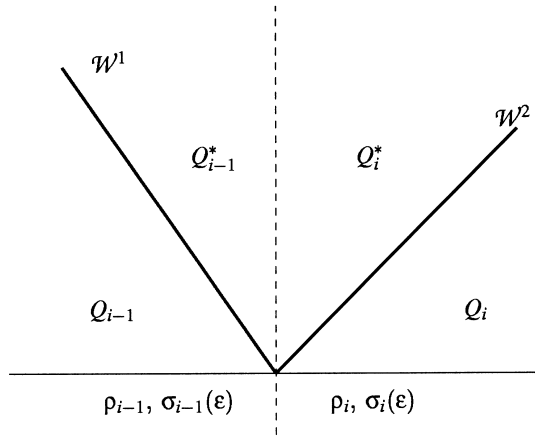


Figure 1. Structure of the Riemann solution.

Similarly, across the two-wave \mathcal{W}^2 we have

$$\begin{aligned} s^2(\varepsilon_i - \varepsilon_{i-1}^*) &= -(u_i - u_i^*) \\ s^2(\rho_i u_i - \rho_i u_i^*) &= -(\sigma_i(\varepsilon_i) - \sigma_{i-1}(\varepsilon_i^*)) \end{aligned} \tag{9}$$

In addition, across the interface at $x_{i-1/2}$ the flux $f(q, x)$ must be continuous for $t > 0$, which requires that

$$\begin{aligned} u_{i-1}^* &= u_i^* \\ \sigma_{i-1}(\varepsilon_{i-1}^*) &= \sigma_i(\varepsilon_i^*) \end{aligned} \tag{10}$$

This makes sense physically since the velocity and stress must be constant across the material interface. If the initial data Q_{i-1} and Q_i have this property then \mathcal{W}^1 and \mathcal{W}^2 will have zero strength. Otherwise, the elastic waves generated are precisely those required to equilibrate the stress and velocity at the interface.

Note that the Riemann solution will generally have a jump in ε and m across the interface. In a sense the Riemann solution consists of four waves: the two propagating elastic waves and two stationary waves at the interface, one having a jump in ε and the other a jump in m . For the wave-propagation algorithms implemented in CLAWPACK, we only need the waves with non-zero speed. Alternatively, for a method implemented in terms of interface fluxes $F_{i-1/2}$, we see that the interface flux is uniquely defined by (10) in spite of the fact that q has a jump at the interface.

To find the exact all-shock Riemann solution, we must determine intermediate states and shock speeds so that the Rankine–Hugoniot conditions (8) and (9) are both satisfied, along with constraints (10). This can be reduced to a non-linear system of two equations for ε_{i-1}^* and ε_i^* since all other quantities can be determined in terms of these. The system is simply (10) after expressing u_{i-1}^* and u_i^* in terms of ε_{i-1}^* and ε_i^* . Combining the two equations from (8)

we can eliminate $u_{i-1}^* - u_{i-1}$ to obtain

$$s^1(\varepsilon_{i-1}^*) = \sqrt{\frac{1}{\rho_{i-1}} \left(\frac{\sigma_{i-1}(\varepsilon_{i-1}^*) - \sigma_{i-1}(\varepsilon_{i-1})}{\varepsilon_{i-1}^* - \varepsilon_{i-1}} \right)} \quad (11)$$

and similarly from (9) we find

$$s^2(\varepsilon_i^*) = \sqrt{\frac{1}{\rho_i} \left(\frac{\sigma_i(\varepsilon_i^*) - \sigma_i(\varepsilon_i)}{\varepsilon_i^* - \varepsilon_i} \right)} \quad (12)$$

This gives the desired relations

$$\begin{aligned} u_{i-1}^* &= u_{i-1} - s^1(\varepsilon_{i-1}^*)(\varepsilon_{i-1}^* - \varepsilon_{i-1}) \\ u_i^* &= u_i + s^2(\varepsilon_i^*)(\varepsilon_i - \varepsilon_i^*) \end{aligned} \quad (13)$$

In principle system (10) can be solved using a non-linear iteration, but in practice a much simpler approximate Riemann solver appears to work well, at least for mildly non-linear problems. This approximate Riemann solver is defined by simply choosing the wave speeds to be the sound speed in the appropriate cell

$$s^1 = -\sqrt{\frac{\sigma'_{i-1}(\varepsilon_{i-1})}{\rho_{i-1}}}, \quad s^2 = \sqrt{\frac{\sigma'_i(\varepsilon_i)}{\rho_i}} \quad (14)$$

If the non-linearity is not too strong, then these are good approximations regardless of the correct values of ε_{i-1}^* and ε_i^* .

For the variable-coefficient linear problem ($\sigma_i(\varepsilon) = K_i \varepsilon$), these expressions are exactly correct and reduce to

$$s^1 = -\sqrt{\frac{K_{i-1}}{\rho_{i-1}}}, \quad s^2 = \sqrt{\frac{K_i}{\rho_i}} \quad (15)$$

For the linear problem we also know that the waves \mathcal{W}^1 and \mathcal{W}^2 must be of the form

$$\mathcal{W}^1 = \alpha^1 r_{i-1}^1 = \begin{bmatrix} 1 \\ Z_{i-1} \end{bmatrix}, \quad \mathcal{W}^2 = \alpha^2 r_i^2 = \begin{bmatrix} 1 \\ -Z_i \end{bmatrix} \quad (16)$$

where Z is the impedance. In this case we can determine α^1 and α^2 by requiring that (10) holds. This is most easily done by defining

$$R = \begin{bmatrix} 1 & 1 \\ Z_{i-1} & -Z_i \end{bmatrix} \quad (17)$$

and solving first the linear system

$$R\beta = f_i(Q_i) - f_{i-1}(Q_{i-1}) \quad (18)$$

for $\beta = (\beta^1, \beta^2)$, thus decomposing the flux difference into $\beta^1 r^1 + \beta^2 r^2$. The waves are then defined by (16) where

$$\alpha^1 = \beta^1/s^1, \quad \alpha^2 = \beta^2/s^2 \quad (19)$$

Note that

$$\mathcal{W}^1 + \mathcal{W}^2 \neq Q_i - Q_{i-1}$$

because there are also other stationary waves at the interface that we have not bothered to explicitly compute. But we do have

$$s^1 \mathcal{W}^1 + s^2 \mathcal{W}^2 = f_i(Q_i) - f_{i-1}(Q_{i-1}) \quad (20)$$

so that the wave-propagation algorithm based on these waves is conservative. We have used the fact that the flux is continuous at the interface to simplify the solution procedure.

Returning to the non-linear problem, we can proceed in the same manner. After choosing s^1 and s^2 by (14), we compute the impedances $Z_{i-1} = -\rho_{i-1}s^1$ and $Z_i = \rho_i s^2$ and then again use the matrix R to solve the system (18). Finally we compute the α 's as in (19) and take the waves to be (16).

Note that the Rankine–Hugoniot conditions will not generally be satisfied across each wave separately in the non-linear case. (The same is true with most approximate Riemann solvers.) However, we continue to have the crucial property (20) so that the wave-propagation algorithm is conservative.

3. NUMERICAL RESULTS

As an example, we consider a periodic medium consisting of alternating layers of two different materials. Each layer is one unit thick. For $2j < x < 2j + 1$ the material has density ρ_A and stress–strain relation $\sigma_A(\varepsilon)$, while if $2j + 1 < x < 2j + 2$ the material is characterized by ρ_B and $\sigma_B(\varepsilon)$. For simplicity each stress–strain relation has the form

$$\sigma(\varepsilon) = K_1 \varepsilon + K_2 \varepsilon^2 \quad (21)$$

We first show some sample results and discuss what is seen. In the next section a grid refinement study is performed for one particular case to verify that the method is converging, with somewhat better than first-order accuracy.

We take initial data $q(x, 0) \equiv 0$ and apply a boundary condition at $x = 0$ of the form

$$u(x, 0) = \begin{cases} -0.2(1 + \cos(\pi(t - 30)/30)) & \text{if } t \leq 60 \\ 0 & \text{if } t > 60 \end{cases} \quad (22)$$

This corresponds to stretching the material by pulling the left edge outward for $0 < t < 60$, leading to an elastic wave propagating through the material. Figures 2–5 show the resulting wave propagation for four different cases. In each case the strain ε and the stress σ are shown as function of x at three different times, with t increasing as one goes upwards through the sequence of plots.

Case I. Homogeneous linear material (see Figure 2)

$$\rho_A = \rho_B = 1, \quad \sigma_A(\varepsilon) = \sigma_B(\varepsilon) = \varepsilon$$

The wall motion creates a cosine-hump acoustic wave that propagates at velocity 1.

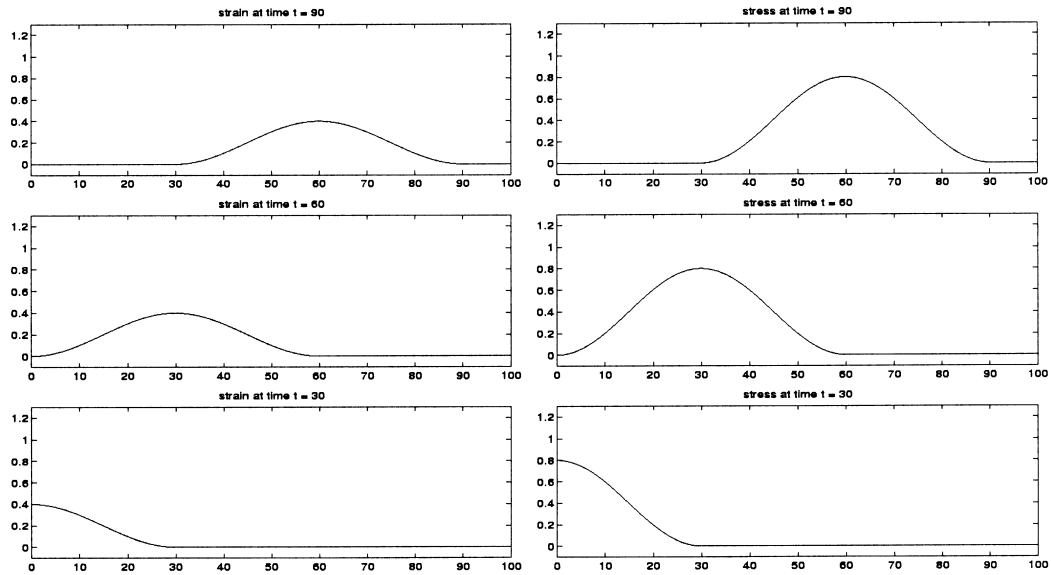


Figure 2. Case I: linear homogeneous medium.

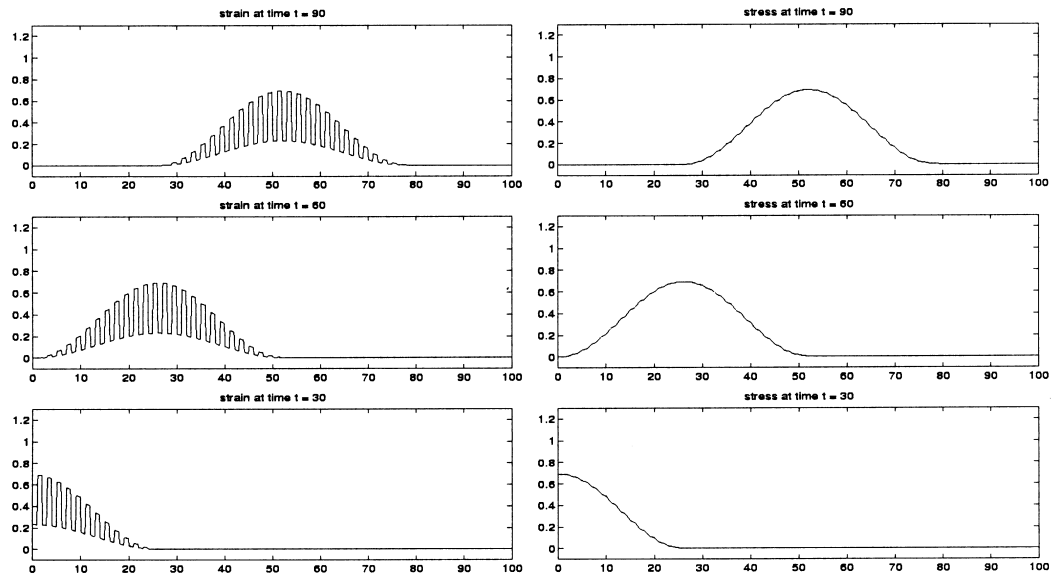


Figure 3. Case II: linear heterogeneous medium.

Case II. Heterogeneous linear material (see Figure 3)

$$\rho_A = 1, \quad \rho_B = 3, \quad \sigma_A(\varepsilon) = K_A(\varepsilon), \quad \sigma_B(\varepsilon) = K_B \varepsilon$$

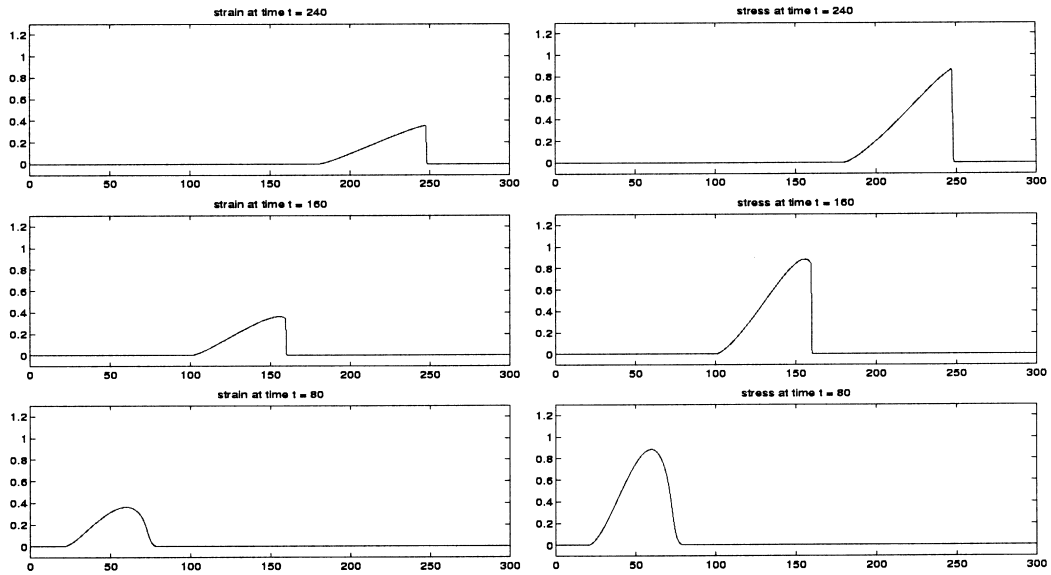


Figure 4. Case III: non-linear homogeneous medium.

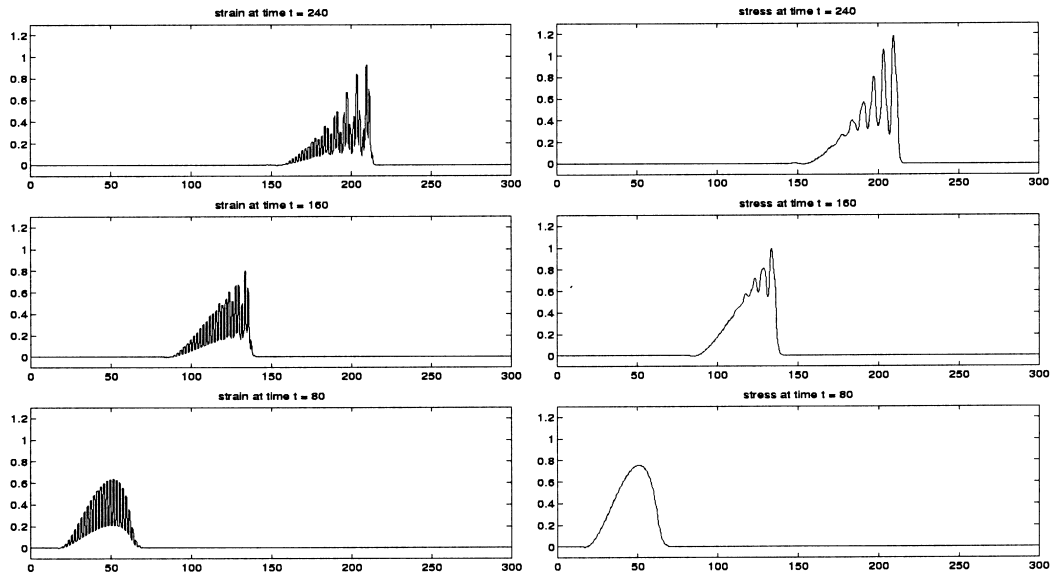


Figure 5. Case IV: non-linear heterogeneous medium.

with $K_A=1$ and $K_B=3$. Again a hump in stress is observed to propagate with a shape that is essentially unchanged. It is not smooth, however. The slope $\sigma_x(x,t)$ is discontinuous at each layer interface, as is the strain $\varepsilon(x,t)$ itself. Note that each material has the same sound speed $c=1$ and yet the wave appears to propagate at a slower speed $\bar{c} \approx 0.866$. This is consistent

with homogenization theory for this problem, which predicts that waves with large wavelength relative to the scale of the heterogeneity will propagate with effective speed $\bar{c} = \sqrt{\hat{K}/\bar{\rho}}$, where $\hat{K} = ((K_A^{-1} + K_B^{-1})/2)^{-1}$ is the harmonic average and $\bar{\rho} = (\rho_A + \rho_B)/2$ is the arithmetic average. Because the impedance is different in the two materials, there is continuous reflection at the material interfaces. The wave does not simply translate but rather bounces back and forth between interfaces, accounting for the slower speed at which the energy propagates. Finite-volume methods based on Riemann solvers are ideally suited to this problem, since solving the Riemann problem at each interface correctly determines the reflected and transmitted portion of each wave.

This case has been studied by Santosa and Symes [9], who derive an effective equation that also contains small dispersive terms. These terms lead to oscillations that can be observed numerically at later times. See Reference [4] for examples and more discussion of this test problem.

Case III. Homogeneous non-linear material (see Figure 4)

$$\rho_A = \rho_B = 2, \quad \sigma_A(\varepsilon) = \sigma_B(\varepsilon) = 2\varepsilon + 1.2\varepsilon^2$$

The non-linearity causes the cosine-hump to steepen into a shock wave followed by a rarefaction wave.

Case IV. Heterogeneous non-linear material (see Figure 5)

$$\rho_A = 1, \quad \rho_B = 3, \quad \sigma_A(\varepsilon) = K_A\varepsilon(1 + 0.3K_A\varepsilon), \quad \sigma_B(\varepsilon) = K_B\varepsilon(1 + 0.3K_B\varepsilon)$$

with $K_A = 1$ and $K_B = 3$. Again the hump in stress begins to steepen, but now oscillations form rather than a true shock wave developing. The long-time behaviour of this solution is particularly interesting, as illustrated further in Figures 6 and 7. The oscillations break up into a series of solitary waves with similar shape but different magnitudes and speeds. The larger waves propagate faster and so they separate further at later times. Moreover, tests where this wave train interacts with another similar wave train suggest that they interact as solitons. This behaviour is consistent with an effective homogenized equation that has the same quadratic non-linear form as (2), but with the addition of a small dispersion term, as might be expected from the linear analysis of [9]. This is reminiscent of the KdV equation with small dispersion, which exhibits similar behaviour (e.g. Reference [10]). In that case a smooth pulse breaks up into a train of solitons with width proportional to the dispersion coefficient.

This non-linear elasticity problem is being investigated further and here we have only shown some preliminary numerical results. In the next section a grid refinement study is shown to demonstrate convergence of the method.

4. ACCURACY

To confirm that the method is converging and estimate the order of accuracy, we solve the problem shown in Figure 5 up to time $t = 240$ using two different grid resolutions. Figures 8 and 9 show the results. In each case the solid line shows the ‘true solution’ as computed on a fine grid with $\Delta x = 0.01$ on the domain $0 \leq x \leq 300$, so there are 100 cells in each of the 300 layers (30 000 grid cells total). Figure 8 shows the results on a grid with $\Delta x = 0.25$ (4 cells per layer) and Figure 9 shows the results on a grid with $\Delta x = 0.125$ (8 cells per layer). In

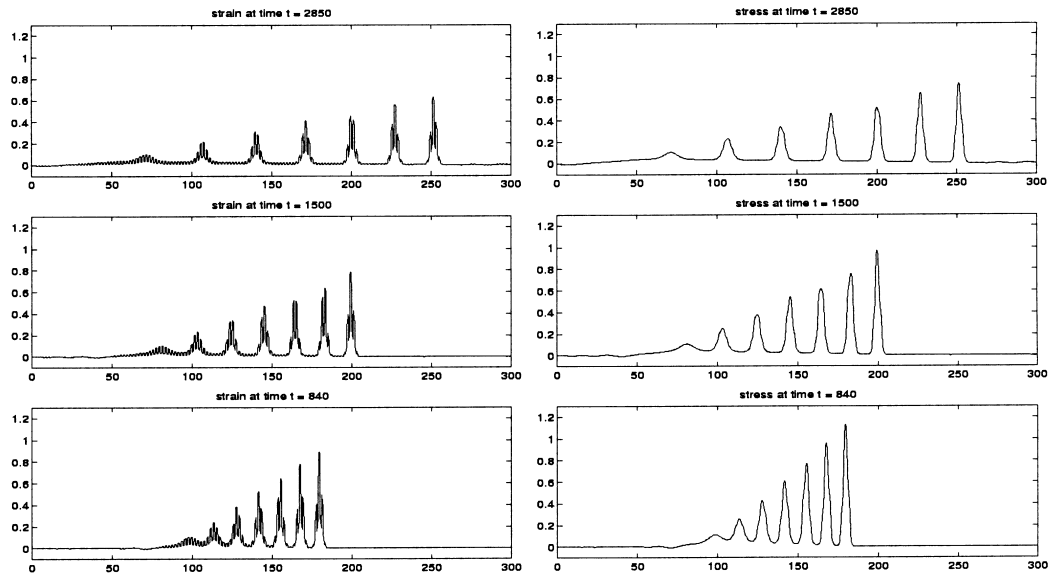


Figure 6. Case IV: non-linear heterogeneous medium, at later times. After time $t=70$ the boundary conditions were switched to periodic boundary conditions so that the wave train continues to cycle through the fixed domain.

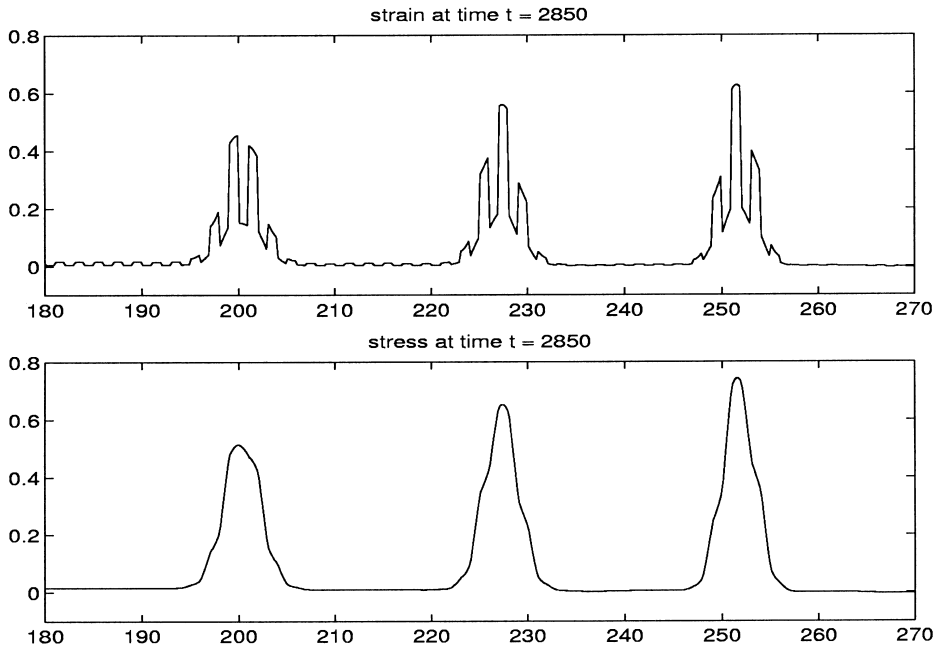


Figure 7. Case IV: non-linear heterogeneous medium. Zoom view of three solitary pulses from Figure 6.

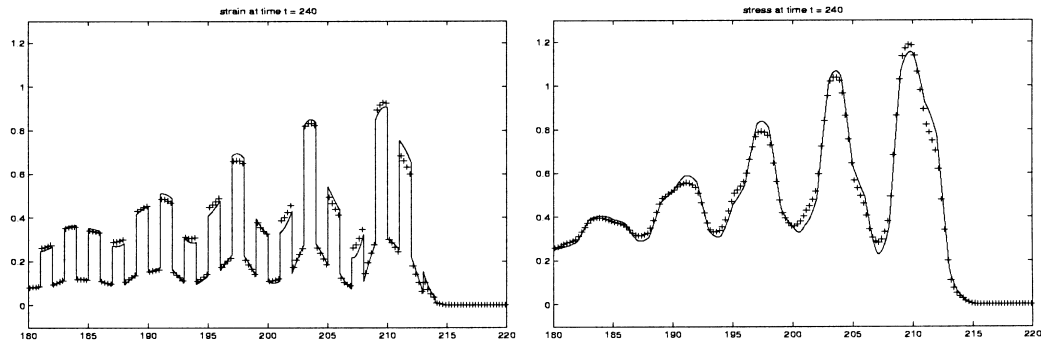


Figure 8. Case IV at time $t = 240$, on a grid with 4 points per layer.

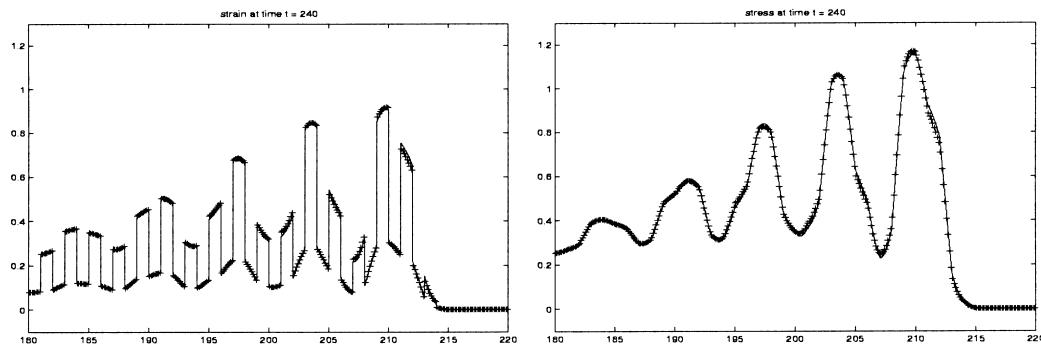


Figure 9. Case IV at time $t = 240$, on a grid with 8 points per layer.

each case the high-resolution wave-propagation algorithm described in Reference [1] is used with the MC (monotonized centered) limiter function. On smooth solutions this method is essentially second-order accurate except near extrema where clipping typically occurs. On the Case IV problem, testing on a sequence of grids shows that the order of accuracy is roughly 1.35 in both the max-norm and the 1-norm. This is reasonable considering that the oscillatory nature of the true solution leads to many extrema.

The strain is computed with essentially the same accuracy as the stress, and both show the same rates of convergence. Note in particular that there is no degradation of the accuracy near the material interfaces where the strain is discontinuous. These discontinuities are not being ‘captured’ by the numerical scheme in the same manner as a moving shock would be. Knowledge of the jumps in the solution at these points is built into the method in the process of solving the Riemann problems. This is a major advantage of Riemann-solver based schemes for problems in heterogeneous media. The Riemann solver can take into account any discontinuities in the solution, as well as properly modelling the reflection and transmission of waves at each material interface.

ACKNOWLEDGEMENTS

This work was supported in part by DOE grant DE-FG03-96ER25292 and NSF grant DMS-9803442.

REFERENCES

1. LeVeque RJ. Wave propagation algorithms for multi-dimensional hyperbolic systems. *Journal of Computational Physics* 1997; **131**:327–353.
2. LeVeque RJ. CLAWPACK software. <http://www.amath.washington.edu/~claw>
3. Fogarty T, LeVeque RJ. High-resolution finite volume methods for acoustics in a rapidly-varying heterogeneous medium. In *Mathematical and Numerical Aspects of Wave Propagation*, DeSanto A (ed.), *Proceedings of the Fourth International Conference on Wave Propagation*, Golden, CO, SIAM: Philadelphia, PA, 1998; 603–605.
4. Fogarty T, LeVeque RJ. High-resolution finite volume methods for acoustics in periodic or random media. *Journal of Acoustical Society of America* 1999; **106**:17–28.
5. Bale D, LeVeque RJ, Mitran S, Rossmannith J. A wave-propagation method for conservation laws and balance laws with spatially varying flux functions. 2002, submitted (<ftp://amath.washington.edu/pub/rj1/papers/vcflux.ps.gz>)
6. Bale D, LeVeque RJ, Rossmannith J. Wave propagation algorithms for hyperbolic systems on curved manifolds. 2002, in preparation.
7. Bardeen J, Buchman L. Numerical tests of evolution systems, gauge conditions and boundary conditions for 1d colliding gravitational plane waves. 2002, submitted.
8. LeVeque RJ, Pelanti M. A class of approximate Riemann solvers and their relation to relaxation schemes. *Journal of Computational Physics* 2001; **172**:572–591.
9. Santosa F, Symes W. A dispersive effective medium for wave propagation in periodic composites. *SIAM Journal of Applied Mathematics* 1991; **51**:984–1005.
10. Lax PD, Levermore CD. The small dispersion limit of the Korteweg–deVries equation. 3. *Communications on Pure and Applied Mathematics* 1983; **36**:809–830.
11. Jin S, Xin ZP. The relaxation schemes for systems of conservation laws in arbitrary space dimensions. *Communications on Pure and Applied Mathematics* 1995; **48**:235–276.